

SHORT COMMUNICATION

## Surface Pressure Estimates for Pitching Aircraft Model at High Angles-of-attack

A. A. Pashilkar

National Aerospace Laboratories, Bangalore–560 017

### ABSTRACT

The surface pressure on a pitching delta wing aircraft is estimated from the normal force and the pitching moment characteristics. The pressure model is based on parametrising the surface pressure distribution on a simple delta wing. This model is useful as a first approximation of the load distribution on the aircraft wing. Leeward surface pressure distributions computed by this method are presented.

**Keywords:** Surface pressure, delta wing aircraft, aircraft wing, load distribution, aerodynamics, vortex breakdown, computational fluid dynamics, surface pressure model, angle-of-attack

### NOMENCLATURE

$a$	Curvature factor of the peak pressure function	$C_{m_{upper}}$	Upper surface contribution to pitching moment
$a_1, a_2$	Surface model parameters for lower surface pressure model	$C_m' \Big _{c_i=0}$	Contribution of camber (residual pitching moment at zero normal force)
$C_m$	Pitching moment	$C_{Z_{body}}$	Body contribution to total normal force
$C_z$	Normal force	$C_{Z_{lower}}$	Lower surface contribution to normal force
$c_r$	Root chord	$C_{Z_{upper}}$	Upper surface contribution to normal force
$\bar{c}$	Mean aerodynamic chord	$k$	Rate of change of shift function with lagged angle-of-attack rate
$C_p$	Coefficient of pressure	$K$	$4.63 \tan^{0.8} \epsilon \tan^{1.2} \cos \alpha / \pi$
$C_{pm}$	Peak surface pressure below vortex core	$x$	Vortex breakdown location under dynamic condition
$C_{p_{max}}$	Peak pressure at wing apex	$x_0$	Vortex breakdown location under static condition
$C_{ps}$	Peak pressure at trailing edge below vortex core	$y$	Coordinate along wing y-axis from apex to the right seen in plan view
$C_{m_{body}}$	Body contribution to total pitching moment	$z$	Height of the vortex core normal to wing surface
$C_{m_{lower}}$	Lower surface contribution to pitching moment		

*Greek Symbols*

- $\alpha$  Angle-of-attack
- $\dot{\alpha}_1$  Lagged angle-of-attack rate
- $\epsilon$  Semi-apex angle-of-the delta wing
- $\tau$  Aerodynamic time constant

**1. INTRODUCTION**

Accurate simple prediction methods like Polhamus<sup>1</sup> suction analogy exist for the estimation of static aerodynamics of aircraft. Traub<sup>2</sup> has developed a prediction method for the longitudinal characteristics, which is also applicable at high angles-of-attack. Certain assumptions about the vortex lift behind the breakdown location have been introduced to account for the phenomenon of vortex breakdown. The results indicate that the method gives good predictive capability at low and moderate angles-of-attack, while the agreement between the model and the experimental data is fair at high angles-of-attack.

Computational fluid dynamics methods<sup>3</sup> or experimental means<sup>4</sup> have been used to obtain the surface pressure distribution. Pashilkar<sup>5</sup> has proposed a method of estimating pressure field corresponding to static conditions on simple delta wings at high angles-of-attack. The approach is based on approximating the leeward surface distribution by suitable functions. It was also shown that the lower surface pressure could be approximated as a linear function of angle-of-attack. The present communication is an extension of this work<sup>5</sup> for unsteady sinusoidal motions of a delta wing aircraft model.

**2. EXPERIMENTAL DATA**

The experimental investigations were carried out in a low speed wind tunnel rig capable of varying the frequency and amplitude of pitch and yaw oscillations in the ranges 0.15Hz to 1.5Hz, and  $\Delta\alpha(\Delta\beta) = 3^\circ$  to  $25^\circ$ . The tests were performed on a delta wing aircraft model with the wing sweep angles close to  $60^\circ$ . Data for the model is available for primary longitudinal coefficients, namely,  $C_z$  and  $C_m$ . The data is in the form of static variation

with angle-of-attack from  $-10^\circ$  to  $60^\circ$  and  $-20^\circ$  to  $20^\circ$  sideslip. A series of large amplitude sinusoidal pitching and yawing experiments were conducted for this configuration at various frequencies and amplitudes in angle-of-attack and sideslip with controls held fixed.

**3. WING/BODY MODEL**

Pashilkar<sup>5</sup> has shown that a surface pressure model based on parametric functions is capable of modelling simple delta wing/body data reported in literature. The total normal force and pitching moment in surface pressure model derived on the basis of component buildup approach are:

$$\left. \begin{aligned} C_{Z\text{Wingbody}} &= C_{Z\text{upper}} + C_{Z\text{lower}} + C_{Z\text{body}} \\ C_{m\text{Wingbody}} &= C_{m\text{upper}} + C_{m\text{lower}} + C_{m\text{body}} + C_m|_{C_z=0} \end{aligned} \right\} \quad (1)$$

Here, the subscripts upper and lower refer to the upper and lower surface contributions to the total coefficient, while the subscript body refers to the contribution from the aircraft fuselage and tailplane. Further, a study of delta wing data revealed the lower surface contribution to be approximately linear with angle-of-attack as

$$\left. \begin{aligned} C_{Z\text{lower}} &= -a_1\alpha \\ C_{m\text{lower}} &= -a_2\alpha \end{aligned} \right\} \quad (2)$$

The expression<sup>5</sup> for the vertical distance  $z$  as a function of the chord-wise coordinate  $x$  and the peak pressure at that location is

$$z = \frac{x4.63 \tan^{0.8} \epsilon \tan^{1.2} \alpha \cos \alpha}{\pi \sqrt{-C_{pm}}} \quad (3)$$

and this expression has been derived from the experimental results of Visser and Nelson<sup>6</sup> and Greenwell and Wood<sup>7</sup>. The peak surface pressure below the vortex core is modelled by the following expression:

$$C_{pm} = (C_{p\text{max}} - C_{ps})(1 - x/c_r)e^{-ax/c_r} + C_{ps} \quad (4)$$

The parameter  $a$  comes into play when vortex breakdown is present on the wing surface.

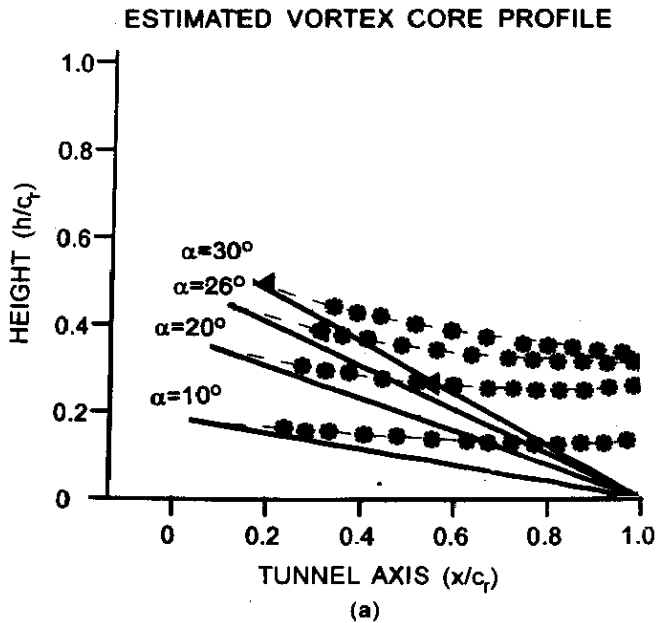


Figure 1(a). Estimated vortex core profile above wing (asterisks show data, dashed lines show model fit, and filled triangles show vortex breakdown position).

This expression is substituted into Eqn (3) and the resulting expression is divided on both sides by root chord ( $c$ ). In this form, it is used to estimate

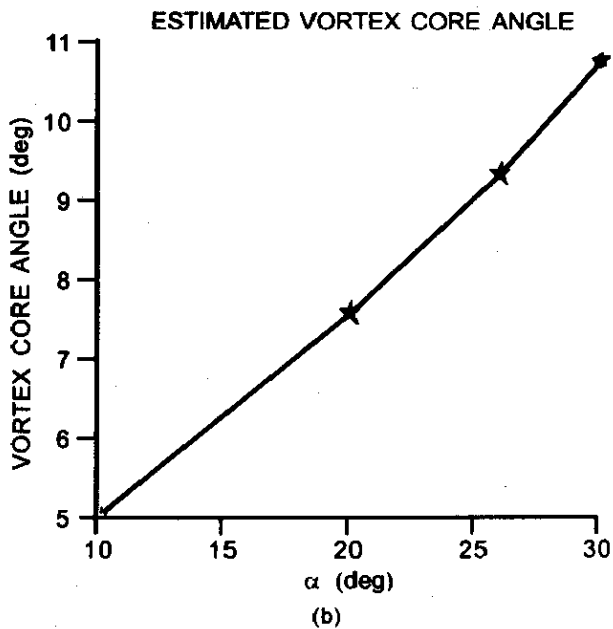


Figure 1(b). Vortex core angle at wing apex at various angles-of-attack.

the non-dimensional vertical location of the vortex core above the  $60^\circ$  delta wing from experimental data. The results for data from Zohar and Er-El<sup>8</sup> are shown in Fig.1(a) marked by asterisks. For comparison, the vortex core height obtained by substituting the actual peak pressure values is also indicated in the figure. The wing profile is shown as a solid line. The match shows that the function represented by Eqn (4) is suitable for modelling the peak pressure under the vortex core from apex to trailing edge.

In Fig.1(b), the side elevation angle of the vortex core axis (the imaginary line that passes through the model apex and estimated vortex core location) is shown as a function of the angle-of-attack. This shows an approximately linear trend with angle-of-attack similar to that in the work of Guglieri and Quagliotti<sup>9</sup>. Finally, the function given by Eqn (4) has the property that when  $C_{p_{max}}$  equals  $C_{ps}$ , the peak pressure distribution becomes a constant. This property is desirable to model the surface pressure after vortex breakdown reaches wing apex. To complete the 2-D surface pressure distribution function on the leeward surface of the delta wing, the (-) variation of the spanwise pressure is postulated as

$$C_p(x, y) = \frac{27}{4} C_{pm}(x) \cdot \left[ \left( \frac{y}{s(x)} \right)^2 - \left( \frac{y}{s(x)} \right)^3 \right] \quad (5)$$

where,  $s(x)$  is the local semi-span.

#### 4. EXTENSION TO PITCHING AIRCRAFT

The variation of the peak pressure at the trailing edge  $C_{ps}(\alpha)$  was assumed to be linear<sup>5</sup> up to the apex breakdown angle-of-attack. A modification of this approach is proposed in this paper for extension to the unsteady response data. The modification consists of a better rationale for modelling of the peak pressure function  $C_{ps}(\alpha)$  at the trailing edge. The static data is modelled first, followed by the unsteady large amplitude sinusoidal response.

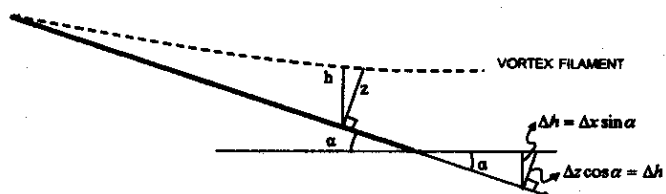


Figure 2. Delta wing in profile

4.1 Static Case

Equation (3) can be rewritten as

$$z = \frac{K \cdot x}{\sqrt{C_{Ps}}} \tag{6}$$

where

$$K = 4.63 \tan^{0.8} \epsilon \tan^{1.2} \alpha \cos \alpha / \pi$$

It is assumed that the vortex line given in terms of the normal distance  $z$  in Eqn (6) leaves the trailing edge in a direction parallel to the free stream (Fig. 2). This gives the following equation:

$$\left. \frac{dz}{dx} \right|_{x=c} = \tan \alpha \tag{7}$$

Substituting Eqn (5) in Eqn (6), differentiating wrt  $x$ , and again replacing in Eqn (7), one obtains:

$$C_{P_{max}} = C_{Ps} \left[ 2e^a \left( \frac{\tan \alpha \sqrt{C_{Ps}}}{K} - 1 \right) + 1 \right] \tag{8}$$

The above expression has been used to model the peak pressure at the apex given its value at the trailing edge. It is seen that the value of  $C_{P_{max}}$  calculated from the above expression can result in the value of  $C_{Ps} < C_{P_{max}}$  itself for low values of angle-of-attack. This is physically meaningless.

To avoid this, the factor  $\tan \alpha \sqrt{C_{Ps}} / K$  is calculated and if found less than unity, it is replaced by 1.01 in Eqn (8). Based on this approximation, the results of estimating the pressure model are shown in Fig. 3 for a delta wing aircraft. In estimating the static data, the pitching moment error between model and data was given more weight than the error in normal force coefficient. This was to ensure the same short period stability prediction from the pressure model. The model matches the pitching moment coefficient accurately, but there are

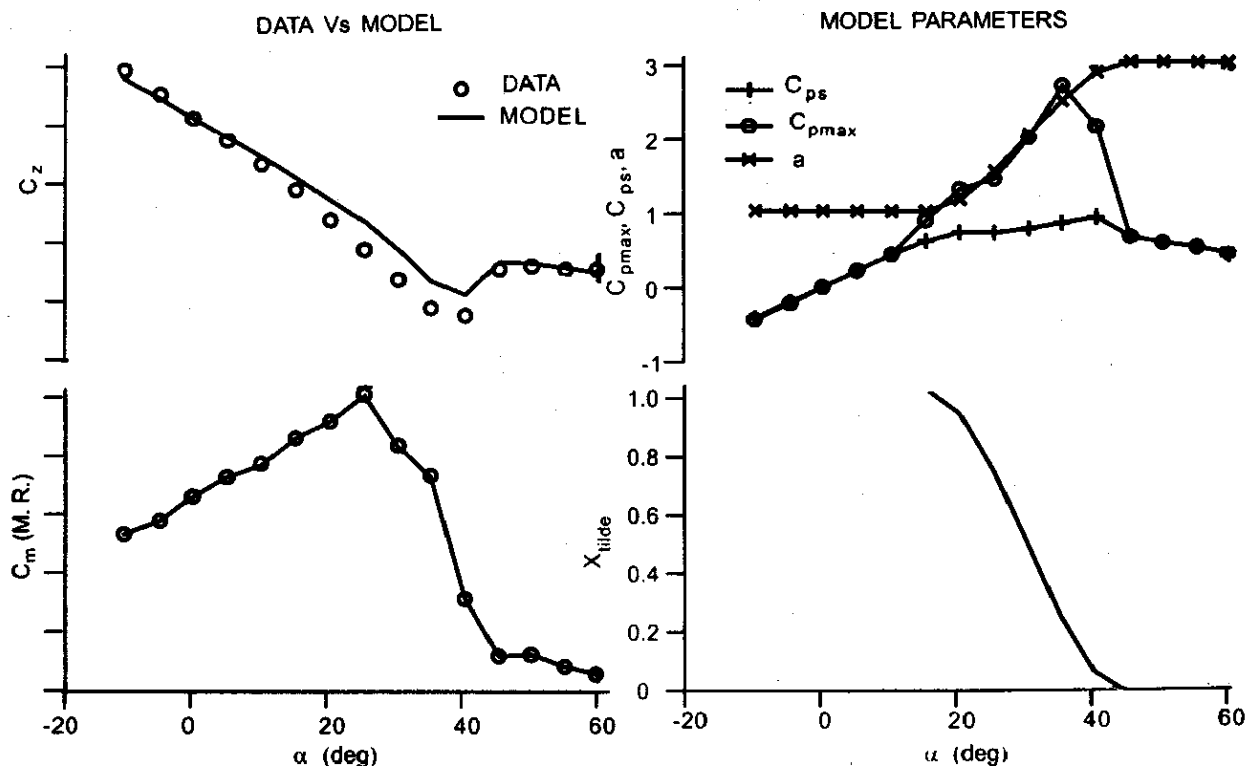


Figure 3. Results of fitting pressure model to static longitudinal data of a delta wing aircraft

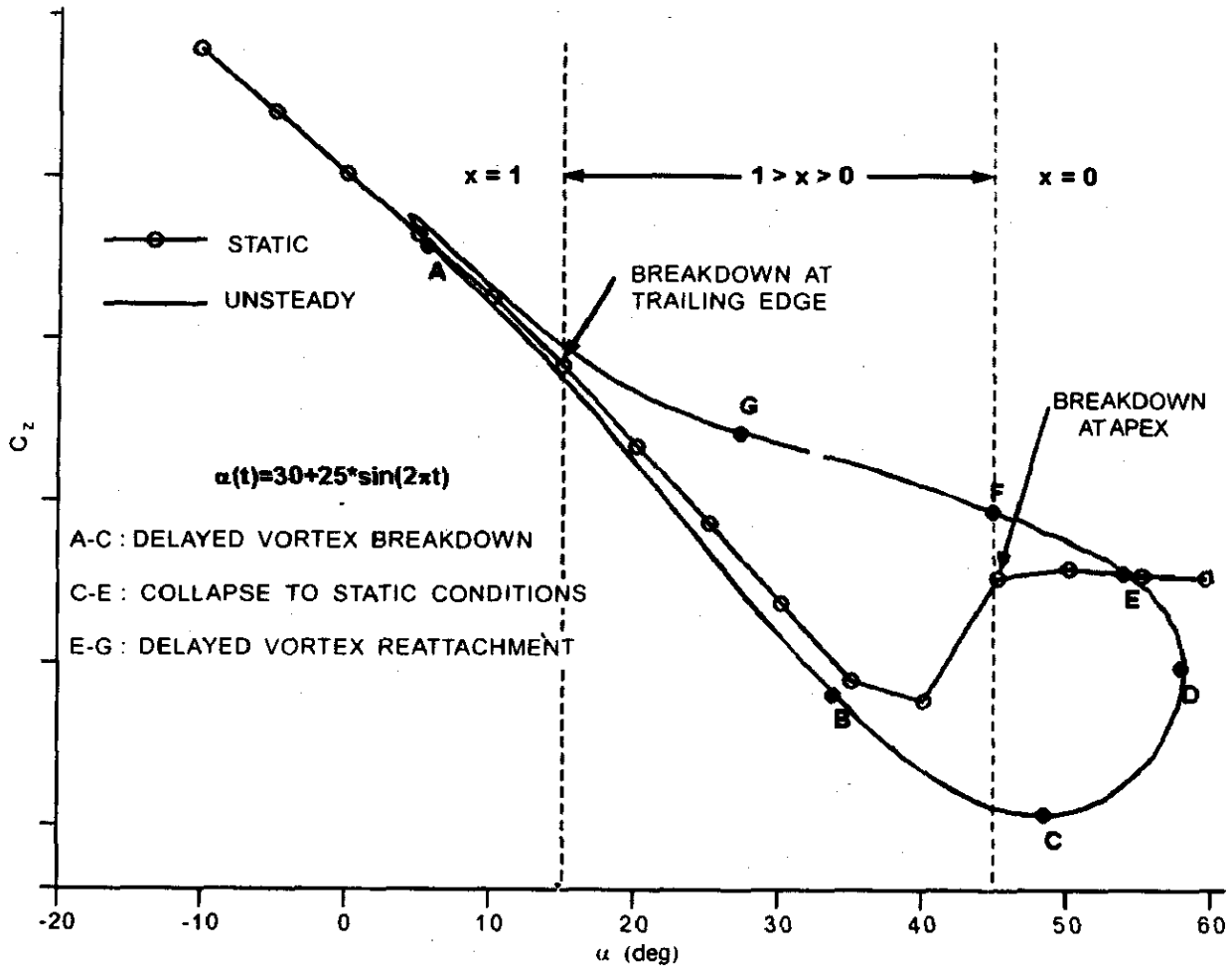


Figure 4. Event cycle during sinusoidal variation in pitch at zero sideslip

differences in the normal force. The difference is attributed to the approximate model for the surface pressure and the fuselage. The fuselage has been obtained from the experimental data of Vishwanath and Patil<sup>10</sup> ( $1/D = 9.8$ ).

The values of lower surface model has been estimated and the estimated values of the constants  $a_1$  and  $a_2$  are 0.0059 and 0.0022, respectively. This compares favourably with the values obtained for Wentz's 60° delta wing data<sup>5</sup>.

#### 4.2 Unsteady Case

The unsteady response of the aircraft consists of a large amplitude oscillations about various mean angles-of-attack at different amplitudes and frequencies. A particular case of the large amplitude response (mean  $\alpha = 30^\circ$

and  $\text{ampl} = 25^\circ$ ) was taken for the study. Knowledge of the static breakdown location with angle-of-attack does not allow to directly determine its variation for the unsteady case. The principal events during a large amplitude cycle have been identified for the normal force coefficient in Fig. 4. It is apparent<sup>11,12</sup> that the breakdown position shows a hysteresis. It has also been shown that the hysteresis is in the form of a lagged rate-dependent shift of the static vortex breakdown<sup>13</sup> position.

$$x(t) = x_0(\alpha - k \cdot \dot{\alpha}_1) \quad (9)$$

where

$$k = \begin{cases} 0.0928, & \dot{\alpha}_1 \geq 0 \\ 0.1258, & \dot{\alpha}_1 < 0 \end{cases}$$

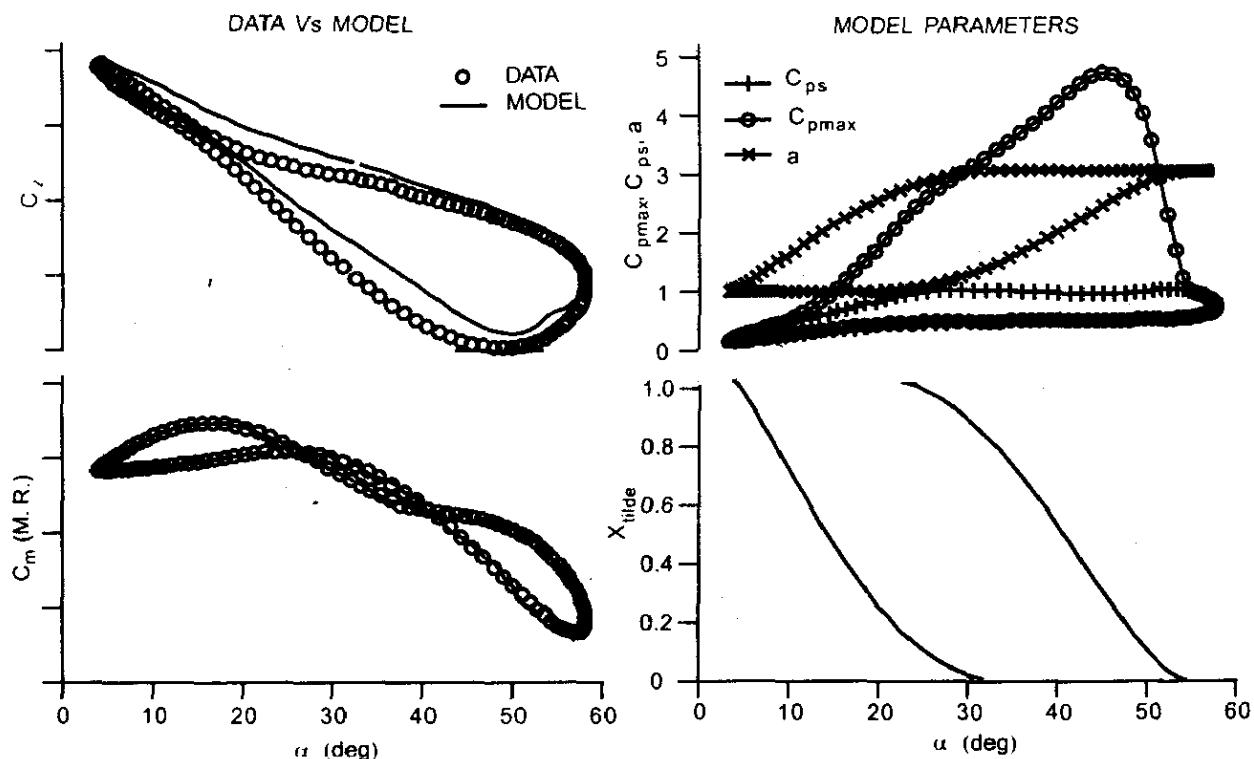


Figure 5. Results of fitting pressure model to LCA unsteady longitudinal data

$$\tau \frac{d\dot{\alpha}_1}{dt} + \dot{\alpha}_1 = \dot{\alpha}(t)$$

The parameters for the vortex breakdown variation given by Eqn (9) have been obtained from the procedure<sup>13</sup>. By generating the time history of vortex breakdown, the dynamic estimation problem can be reduced to a static optimisation problems. The estimation results of the unsteady surface pressure parameters are presented in Fig. 5. It is seen that the model parameters are plausible. The match in pitching moment coefficient is excellent, while the normal force coefficient match is reasonable.

### 5. 3-D VIEW OF SURFACE PRESSURE

The leeward surface pressure estimate on the right half-wing (other half is similar) for the static data is shown in Figs 6(a) and 6(b) for the range of angles-of-attack from 4.86° to 33.2° and 35.1° to 55.2°, respectively. The surface pressure corresponds to the parameters shown in Fig. 3. The pressure surfaces are as viewed from behind the trailing edge with an azimuth of

60° and elevation of 45°. In these figures, the root chord and the semi-span of the wing is non-dimensionalised by the root chord. The key features are the appearance of vortex breakdown at about 15° angle-of-attack (modelled as a flattening of the surface pressure<sup>14</sup>). Vortex breakdown is seen to move in and reach apex at about 45° angle-of-attack.

In Figs 7(a) and 7(b), the surface pressure distributions are shown for the sinusoidally pitching aircraft model during the pitch-up phase. The surface plot corresponds to the parameters estimated in Fig. 5. It is seen that vortex breakdown does not occur on the wing surface till about 33° angle-of-attack and reaches wing apex at 55° angle-of-attack. When these figures are compared to the static pressure distribution as shown in Figs 6(a) and 6(b) for the same incidences, it is clear that vortex breakdown is shifted to a higher angle-of-attack during pitch-up. The opposite effect is seen in the estimates of the surface pressure distribution during pitch-down [Figs 8(a) and 8(b)]. It is noted that vortex

PASHILKAR: SURFACE PRESSURE ESTIMATES FOR PITCHING AIRCRAFT

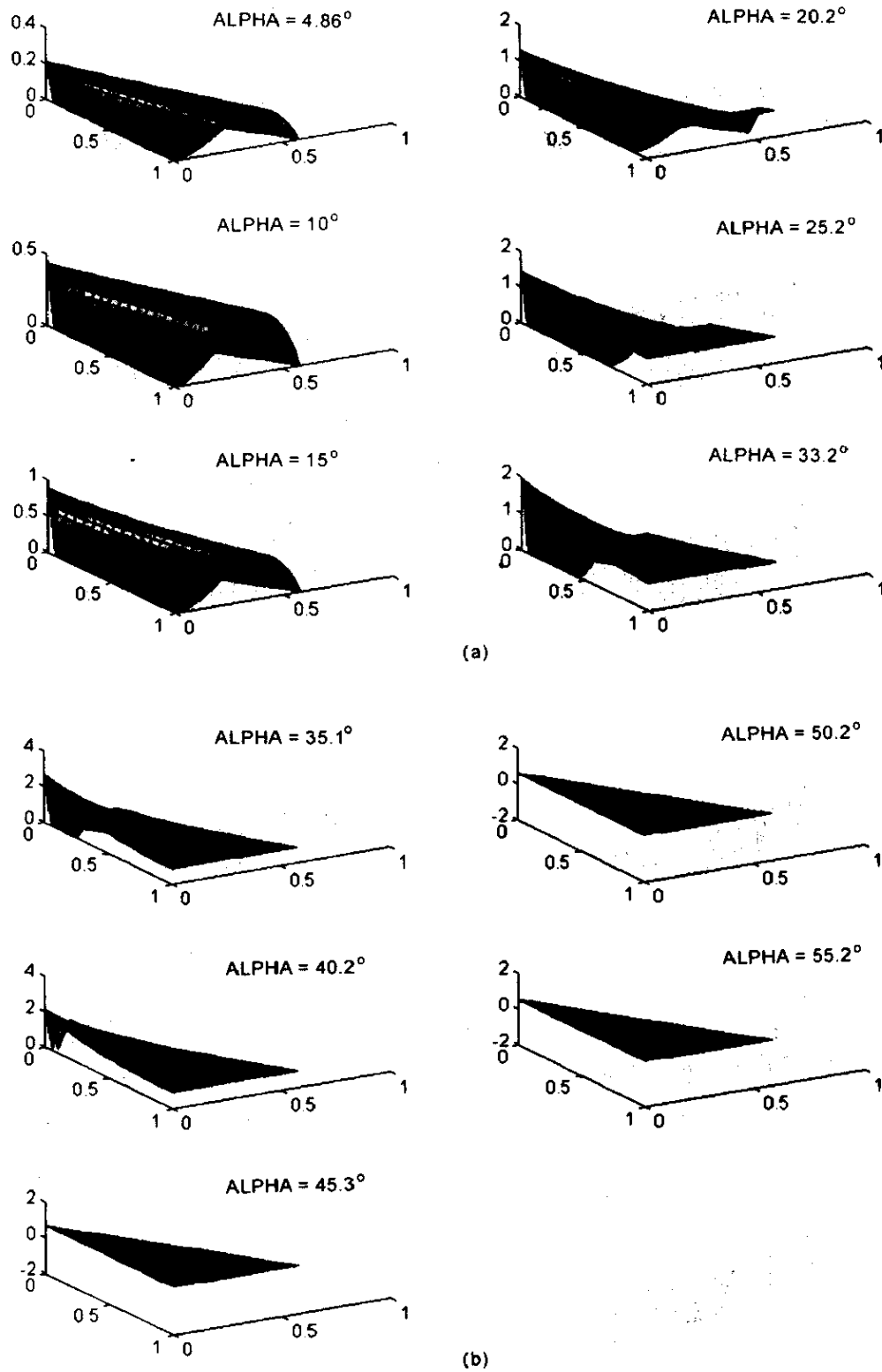


Figure 6. Leeward pressure on half-wing at static condition (a) 4.86° AOA to 33.2° AOA and (b) 35.1° AOA to 55.2° AOA

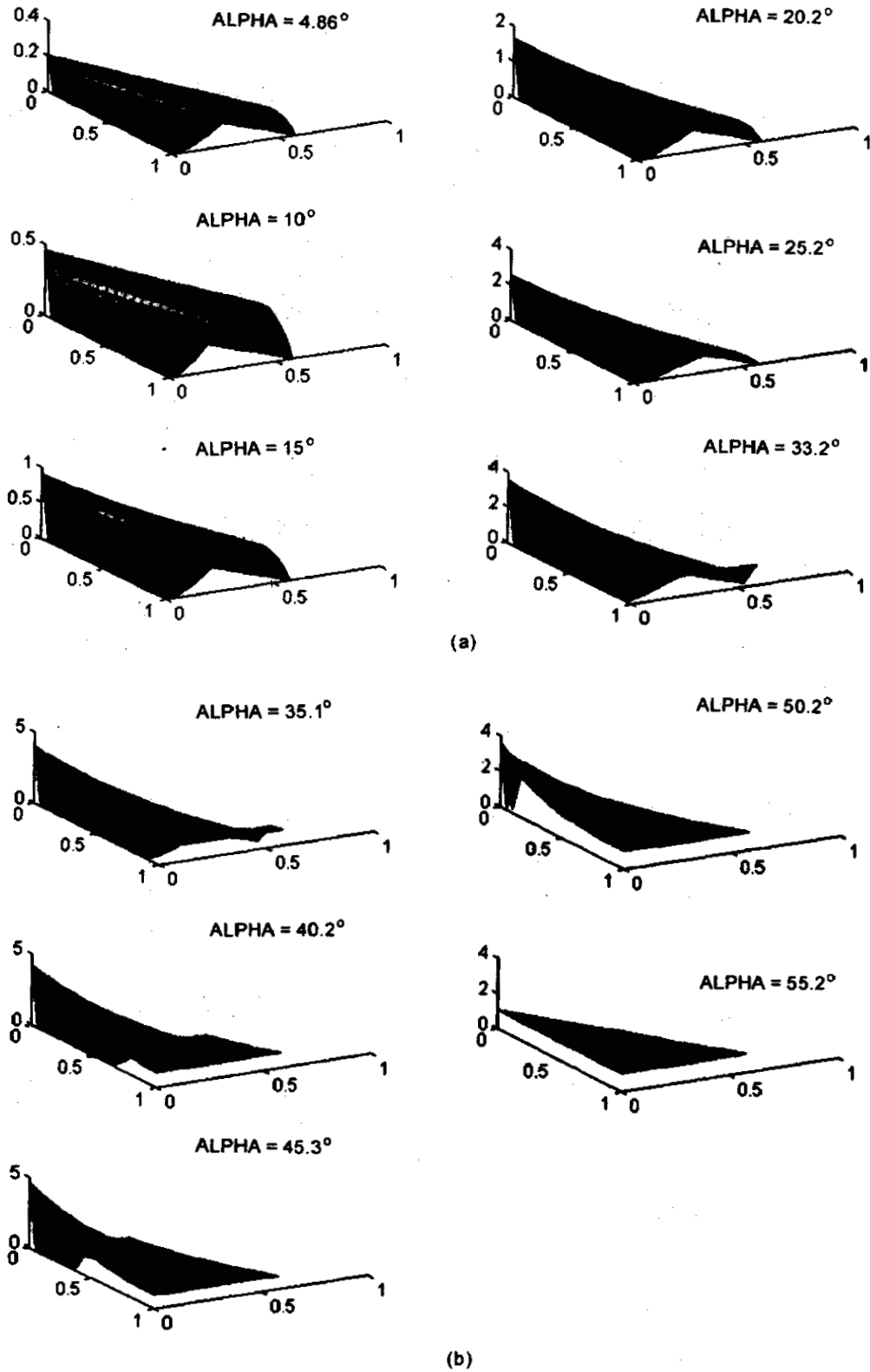


Figure 7. Leeward pressure on half-wing during pitch-up (a) 4.86° AOA to 33.2° AOA and (b) 35.1° AOA to 55.2° AOA

PASHILKAR: SURFACE PRESSURE ESTIMATES FOR PITCHING AIRCRAFT

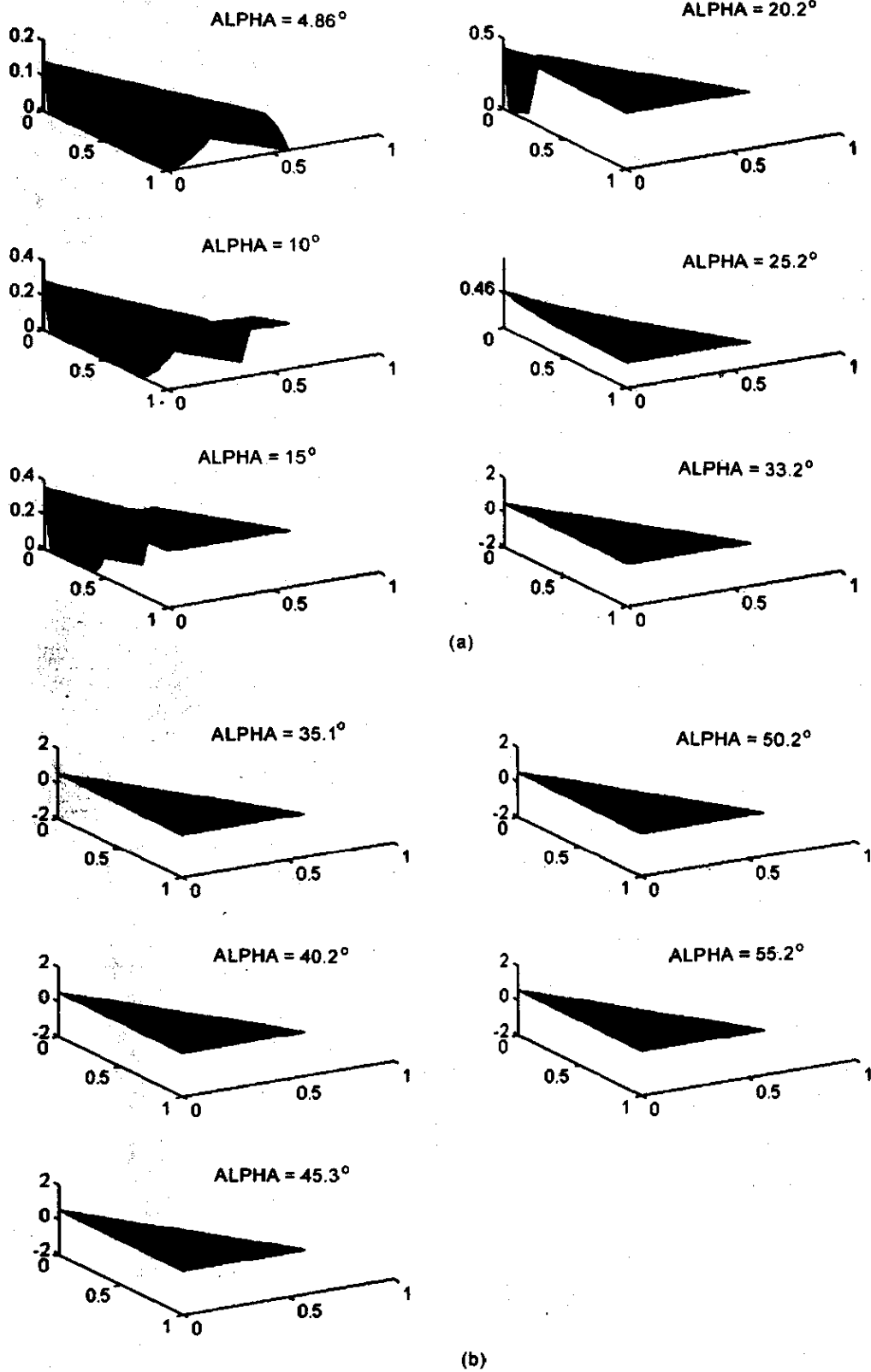


Figure 8. Leeward pressure on half-wing during pitch-down (a) 4.86° AOA to 33.2° AOA and (b) 35.1° AOA to 55.2° AOA

breakdown location does not begin moving towards the trailing edge till the wing has reached an angle-of-attack of  $20^\circ$ .

## 6. CONCLUSION

A new approach to estimate the delta wing surface pressure distribution has been extended to the unsteady variation for sinusoidal pitching aircraft. The modelling structure is simple and capable of estimating the surface pressure distribution for the unsteady case after suitably accounting for the vortex breakdown location variation. A good match has been shown between model and experimental data for normal force and pitching moment of a delta wing aircraft with sweep close to  $60^\circ$ .

## REFERENCES

1. Polhamus, E.C. A concept of the vortex lift of sharp-edge delta wings based on a leading edge suction analogy. Report No. NASA-TN-D-3767, December 1966.
2. Traub, L.W. Prediction of vortex breakdown and longitudinal characteristics of swept slender planforms. *Journal of Aircraft*, 1997, **34**(3), 353–59.
3. Hoeijmakers, H.W.M. Methods for numerical simulation of leading edge vortex flow. In Proceedings of the Symposium on Vortex-Dominated Flows, 9–11 July 1985. NASA Langley Research Centre, Hampton, VA. pp. 223–69.
4. Yegna Narayan, K. & Seshadri, S.N. Types of flows on the leeward side of delta wings. *Prog. Aerospace Sci.*, 1997, **33**.
5. Pashilkar A.A. Surface pressure model for simple delta wings at high angles-of-attack. 19<sup>th</sup> Applied Aerodynamics Conference, 11–14 June 2001. American Society for Aeronautics and Astronautics, Anaheim, CA. AIAA Paper No. 2001–2415.
6. Visser, K.D. & Nelson, R.C. Measurements of circulation and vorticity in the leading-edge vortex of a delta wing, *AIAA Journal*, 1993, **31**(1), 104–11.
7. Greenwell, D.I. & Wood, N.J. Determination of vortex burst location on delta wings from surface pressure measurements. *AIAA Journal*, 1992, **30**(11), 2736–739.
8. Zohar, Y. & Er-El, J. Influence of the aspect ratio on the aerodynamics of the delta wing at high angle-of-attack. *Journal of Aircraft*, 1988, **25**(3), 200–05.
9. Guglieri, G. & Quagliotti, F.B. Experimental investigation of vortex dynamics on a  $65^\circ$  delta wing in sideslip. *Aeronautical Journal*, March 1997, 111–20.
10. Vishwanath, P.R. & Patil, S.R. Aerodynamic characteristics of delta wing-body combinations at high angles-of-attack. National Aerospace Laboratories (NAL), Bangalore. Report No. NAL-PD EA 9205.
11. LeMay, S.P.; Batill, S.M. & Nelson, R.C. Vortex dynamics on a pitching delta wing. *Journal of Aircraft*, 1990, **27**(2), 131–38.
12. Thompson, S.A.; Batill, S.M. & Nelson, R.C. Separated flowfield on a slender wing undergoing transient pitching motions. *Journal of Aircraft*, 1991, **28**(8), 489–95.
13. Pashilkar, A.A. Flow incidence rate model for unsteady aerodynamics at high angles of attack. In 19<sup>th</sup> Applied Aerodynamics Conference, 11–14 June 2001. American Society for Aeronautics and Astronautics, Anaheim, CA. AIAA Paper No. 2001–2469.
14. Myatt, J.H. & Arena, A.S.(Jr). A theoretical/empirical model for rolling delta wings with vortex breakdown. AIAA Paper No. 98–2527, 1998.